Mechanical and optical properties of the femoral chordotonal organ in beetles (Coleoptera)

Leonid Frantsevich[1],*, Irina Shumakova[2] and Dmytro Gladun[2]

ABSTRACT

The femoral chordotonal organ (FCO) in beetles differs from that in orthopterids in the origin of its apodeme: it originates directly from the tibia in the latter, but amidst the tendon of the extensor muscle in the former. In many beetles, the apodeme pops up from the tendon as a short sclerite (arculum). It turns distally upon bending of the tibia. The turn of the arculum is several times more than the turn of the tibia, and the arculum is connected to the FCO. This system behaves as a high-pass filter with a time constant close to the step period. Various aspects of the arculum have been studied previously, including its shape in various taxa, its biomechanics, matched neural activity in the FCO, as well as evolutionary aspects. The results of previous studies, published in 1985–2003 in Russian, are inaccessible to most foreign readers. However, original texts and the list of studied species (>350) are now available online. Recently, we minimized the system to three components: the proximal tibial ledge, the tendon and the arculum. The elastic tendon contains resilin. In four model species, the arculum readily turned upon stretching of the tendon. Turning was video recorded. The force of approximately 0.005 N, applied to a tendon approximately 0.25 mm in size, is enough for the utmost turn of the arculum. The arculum turned also upon local deformations close to its base. The ability to turn vanished after incision between the arculum and the distal part of the extensor apodeme. A mechanical model of an amplifier is proposed. The apodeme includes optically active structures, which behave differently in polarized light.

KEY WORDS: Extensor tendon, Arculum, Angular amplification, Resilin, Optical activity

INTRODUCTION
Femoral chordotonal organs in beetles

Femoral chordotonal organs (FCO) measure an angle in the femoro-tibial joint (FTJ). The FCO was discovered in the grasshopper *Melanoplus differentialis* by Slifer (1935). Physiology of the FCO was thoroughly studied in the locust *Schistocerca gregaria*, the stick insect *Carausius morosus* and related species. Here, we discuss mechanical aspects of the FCO.

The neural part of the FCO in orthopterids is connected directly with the tibia via a long rod-like apodeme (Bässler, 1965, 1967; Burns, 1974; Burrows, 1987; Shelton et al., 1992; Usherwood et al., 1968). This apodeme is the invagination of the external integument.

[1]Schmalhausen-Institute of Zoology, National Academy of Sciences of Ukraine, Kiev 01601, Ukraine. [2]Institute for Evolutionary Ecology, National Academy of Sciences of Ukraine, Kiev 03143, Ukraine.

*Author for correspondence (frantsevych@nas.gov.ua)

L.F., 0000-0002-3042-3392; I.S., 0000-0001-6512-6593; D.G., 0000-0003-1640-2488

The FCO apodeme lies parallel to the apodeme of the musculus extensor tibiae (MET). The MET apodeme invaginates inside the femur as a long flat band for attachment of myofibrils. Excursions of the tibia inside the femur are transmitted via a rod-like apodeme to the neural part of the FCO. A similar origin of the apodeme was reported for the moth *Manduca sexta* (Lepidoptera) by Kent and Griffin (1990), cited in Field and Matheson (1998), and for the hornet *Vespa crabro* (Hymenoptera) (Shumakova, 2003, fig. 2A).

I.S. and L.F. have studied the FCO apodeme of beetles since the 1980s. The separate origin of the FCO apodeme from the arthrodial membrane is not conspicuous in beetles. A free sclerotized rod of the FCO apodeme gets outside in the middle of the tendon of the MET apodeme and continues its way to the FCO. A hollow channel from the tibia to the base of a rod was noticed in some whole mounts of the tendon or in histological slides. However, in 20–25% of beetle species, the rod appears as a short sclerotized club – straight (in Adephaga) or curved (in Polyphaga) – which continues proximally as a soft ligament in Adephaga or several ligaments in Polyphaga. Results of these studies have been published in Russian and are still unknown abroad. We provide below a concise review of these observations. Photocopies of original publications and the list of >350 inspected beetle species are available online at http://izan. kiev.ua/ppages/frantsevich/arc.htm or from the reference list for particular articles.

A curved club (a small arch, or the arculum) was firstly found in *Lethrus apterus* (Geotrupidae; Lethrinae). The schematic positions of the MET and FCO in the femur is depicted in Fig. 1A (Frantsevich and Shumakova, 1985, fig. 1). Typical arcula are depicted in Fig. 1C–F. We apply the term 'arculum' both to straight or curved clubs. We refer to the connection of the arculum with the tendon as the base of the arculum, and the free end is referred to as the tip.

We observed the arculum in an amputated leg via a small window in the anterior wall of the femur (Fig. S1A; from Frantsevich and Shumakova, 1987a, fig. 5A). Astonishingly, the arculum responded to a small flexion of the tibia with a quick turn distally. When the dorsal ledge of the tibia inside the femur moved distally, the arculum turned distally as well. Turns of the tibia were exerted with a pen recorder, coaxial with the FTJ and operated by a pulse generator. Turns of the arculum were recorded with a video kymograph on a running film as a trace of the arculum across a scan line of a video image (Fig. S1B; from Frantsevich and Shumakova, 1985, fig. 2). The scan rate was 25 s^{-1}. The trace reproduced sinusoidal oscillations of the arculum (Fig. S1C–F) or a response to rectangular pulses.

The amplitude of the illustrated tibial oscillations was 0.4 deg. Turns of the arculum appeared several times wider than turns of the tibia. For the femoro-tibial angle in the sector of 60–80 deg, oscillations above 2–3 Hz at the tip of the arculum in *L. apterus* were 15-fold larger than at the base. At 10 Hz, the ratio between angular excursions of the tibia and the arculum was 1:25. Angular amplification diminished at frequencies below 2 Hz. The response to a stepwise turn decayed exponentially with a time constant of
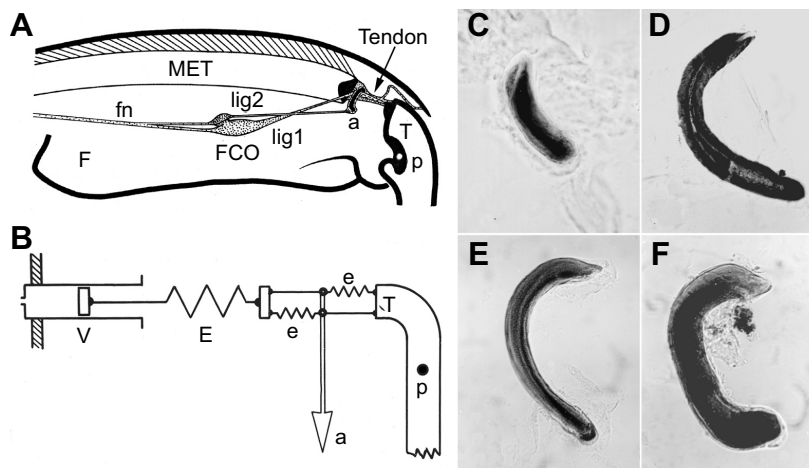
Fig. 1. The femoral chordotonal organ (FCO), musculus extensor tibiae (MET) and arculum in beetles. (A) MET and FCO in the femur of *Lethrus apterus*; (B) a visco-elastic model of the arculum suspension. Separated arcula in (C) *Calosoma inquisitor*, (D) *L. apterus*, (E) *Pentodon idiota* and (F) *Chalcophora mariana*, not to scale. a, arculum; E, e, elastic springs; lig1, lig2, ligaments from the base and the tip of the arculum to FCO; p, pivot of the femoro-tibial joint; V, viscous element. Arrows in B show leg-fixed axes.

0.4–0.5 s. The step frequency in *L. apterus* was approximately $2\,\mathrm{s}^{-1}$. A more important index is displacement of the tip by 150–170 µm per 1 deg of turn of the tip; it is equivalent to the signal transmitted to the FCO via the ligament (Frantsevich and Shumakova, 1985). Performance of the arculum in *L. apterus* appeared the best among several tested beetles (Table S1).

Responses in *L. apterus* diminished at both sides out of the optimal joint angle (Frantsevich and Shumakova, 1987a, fig. 4). During the stepwise extension, amplification by the arculum was optimal at the FTJ angle of 75 deg; however, during the reverse flexion, maximal sensitivity shifted to 60 deg (histeresis). This was caused presumably by two factors: (1) bending of the internal head of the tibia and change of leverage and force applied to the extensor tendon at different angles of the FTJ (Heitler, 1974) and (2) viscosity in the myofibrils in the leg.

The simplest explanation of high-pass filtering is Maxwell's model (Brankov, 1981) of an elastic and a viscous element in series (Fig. 1B; from Frantsevich and Shumakova, 1987a, fig. 6). However, real elastic and viscous elements were not identified.

Development of the equation is given in Frantsevich and Shumakova (1987a). Lengthening of the elastic element is directly proportional to applied force, whereas proportionality in the viscous element refers to velocity of lengthening, which is the first time derivative. The ratio between the amplitudes at the tip and the base of the arculum, or gain G, depends on frequency. The optimal value for the time constant was fitted to obtain the least square deviation of the computed gain from real values (Frantsevich and Shumakova, 1987a, fig. 2, eqns 1–8). We obtained optimal values for the time constant $\tau=0.435$ s, and for the gain $G=16.12$. The other way to evaluate the time constant is to measure the exponential response of the arculum to a quick (step-wise) turn of the tibia.

Electrophysiological records on a large scarab *Scarabaeus transcaspicus* were published in a short communication (Shumakova, 1989, fig. 2). She recorded the summary electrical activity in the anterior femoral nerve, which included axons from two scoloparia of the FCO. Each one is linked with one of the ligaments. These ligaments were separated from the arculum. A single branch (∼6 mm long) was glued to a glass microcapillary with *n*-butyl-2-cyanoacrylate (B. Braun, Germany). The capillary was attached to the pen of the recorder, mentioned above. Sinusoidal mechanical stimuli below 10 Hz were applied. Bursts of spikes in the anterior femoral nerve coincided with the phases of maximal velocity of deformation, similarly at contraction or stretching. Some directionally sensitive units were active only at one phase of deformation. The higher the amplitude of oscillation, the higher the number of spikes in the burst. A step-wise stimulus exerted a burst of spikes, similarly at stretch or release of the ligament. Responses from both ligament branches were similar. It is likely that the specificity of information in each part of the FCO originated at the mechanical level.

In a second short communication (Shumakova, 1990), histology of the FCO and the arculum was studied in *L. apterus*, the carabids *Carabus cancellatus* and *Cicindela maritima*, and the ladybird *Coccinella septempunctatum* on semi-thin sections of epon-812 embedded femora, stained with Toluidine Blue. Whole mounts of the FCOs of the carabid *Anthia mannerheimi*, the stag beetle *Lucanus cervus* and the scarab *Scarabaeus transcaspicus* were processed in the same fashion. Specimens were viewed using a phase-contrast microscope. The author observed a thin channel inside the tendon of the MET, which led to the base of the arculum. Scolopidia in the FCO were also illustrated. Longitudinal lamellae with radially oriented cross-sections ∼15 µm wide were observed at the base of the arculum in *L. apterus*.

Laboratory studies were completed with a broad search of the arcula in over 350 species of 84 beetle families (Frantsevich and Shumakova, 1987b). As the arculum remained well preserved in dry specimens, we also searched museum collections.

Well-developed arcula were found in almost all Adephaga (eight families). A sole ligament emerged from the tip of the straight arculum. Arcula in Polyphaga, if present, are curved and develop two or more ligaments to the FCO. Well-developed arcula are obligate for all Scarabaeiformia and some Elateriformia (formerly Dascilliformia; i.e. in Buprestidae, Rhipiceridae, Byrrhidae, Heteroceridae and two archaic subfamilies of Elateridae); they are seldom seen in Cucujiformia, but are present in all Coccinellidae (and uncertainly in Cerylonidae; personal communication, R. A. Crowson, Zoology Department, University of Glasgow).

On the contrary, no arculum was found in Cupedidae (Archostemmata), five families of Staphyliniformia, 15 families of Elateriformia, four families of Bostrychiformia, or 38 families of Cucujiformia, including Tenebrionodae, Cerambycidae, Chrysomelidae and Curculionidae.

We traced some cases of presumable reduction of the arculum: large but immobile in Dytiscidae or absent in some dytiscid subfamilies and Gyrinidae in Adephaga; absent in five advanced elaterid subfamilies; and proportionally tiny in the elateriform families Byrrhidae and Rhipiceridae. Thus we concluded that approximately 90,000 among 400,000 beetle species possess the arculum.

In Frantsevich and Shumakova (1987b), we illustrated shapes of arcula in over 150 beetle species (http://mail.izan.kiev.ua/frants/EnRev.pdf, http://mail.izan.kiev.ua/frants/Plates.pdf). The list of all inspected species and indication of the size of the arculum, if present, is accessible as a table in Excel format at http://mail.izan.kiev.ua/frants/TOTAL.xls. We did not match the existence and development of the arcula with phylogenetic schemes for Coleoptera. But we did discuss probable stages of the functional evolution in the FCO apodeme (Frantsevich and Shumakova, 1993, fig. 4).

The best-developed arculum, as far as we know, belongs to *L. apterus*. This species digs holes with larval cells, makes long pedestrian excursions for leaflets, forms packets of leaflets and promptly walks backwards. Other Geotrupinae (Geotrupidae) and Scarabaeinae (Scarabaeidae) also demonstrate similar behavior. Further, stag beetles (Lucanidae) and bess beetles (Passalidae) spend most of their time under bark, nursing larvae and excavating tunnels. These beetles have well-developed arcula.

In contrast, arcula are present in less-talented chafers (Melolonthinae: Scarabaeidae), archaic click beetles (Cardiophorinae and Tetralobinae in Elateridae) and Heteroceridae. Well-developed arcula are obligate in jewel beetles (Buprestidae), with a rather simple usage of legs by imagines. What is puzzling is the possession of well-developed arcula by all ladybirds (Coccinellidae), which may be unique among the Cucujoidea. The series of early studies left the real mechanism of the arculum motility unsolved and did not match unambiguously the mechanical complexity of the arculum against real behavioral demands in a given coleopteran taxon.

Study objectives
Our localization of elastic and viscous elements in Maxwell's model was tentative. Hence, we decided to study a minimal system of three components: the MET apodeme (without myofibrils), the arculum and the MET tendon. We excluded myofibrils as passive viscous elements and identified the localization of elastic elements. In these experiments, we applied stretch directly to the tendon. We propose a simple mechanical model based on video records.

MATERIALS AND METHODS
Leg-fixed coordinate system
The six legs of an insect are oriented differently with respect to the body. We use names for directions that fit any leg. Let us bend (in imagination) the femur and the tibia at a right angle and construct the leg plane across three joints: femoro-tibial, tibio-tarsal and coxo-trochanteral. Let the leg plane be placed at a right angle to the fore–aft body axis, the femur points laterally. Here, we recognize three invariant pairs of directions: anterior–posterior, dorsal–ventral and proximal–distal.

Insects
Beetles were collected in the Kiev Region (Ukraine) and stored either in a freezer or in 70% ethanol. Separated legs were glued posterior face up to a rubber scaffold. Legs were dissected in a drop of ethanol using a sliver of a hard razor and forceps (Fisher Scientific, A. Dumont & Fils, Switzerland) under an MBS-9 stereomicroscope (LOMO, former USSR). The MET was exposed without damage to the anterior face of this muscle. The dorsal ledge of the tibia was separated from the rest of the tibia. The whole muscle together with the tibial ledge was placed in 70% ethanol. Myofibrils were plucked off.

Plucked specimens were stored in drops of glycerol and mounted on microscope slides in the glycerol–chloral hydrate–gum medium. Specimens, stored in glycerol, retained their ability to respond with turns of the arcula to stretch of the tendon, either after transfer into 70% ethanol or as suspended in the air with residual glycerol lubrication.

Some beetles were obtained from old collections. Their legs were macerated in 70% ethanol before dissection. In total, more than 250 whole mounts of muscles from 23 species were inspected. Species mentioned in the text are listed in Table S2.

Photography
Specimens were photographed using the following microscopes. (1) MBS-9 with a Canon EOS 550D camera. Whole mounts were submerged in 96% ethanol, in order to neutralize reflections, and illuminated at a skew against the blue or black background. (2) Olympus CX41s with a Canon EOS 600D. (3) Olympus BX 51 with a WU filter (excitation 330–385 nm, 420 nm longpass emission filter) and a Canon EOS 600D. The presence of resilin-like proteins was inferred in places with blue autofluorescence. (4) LOMO MBI-3 with a Canon EOS 550D, equipped, if necessary, with two polarization filters, inserted above the condenser and above the ocular. Two positions of filters were used: with parallel orientations of E-vectors or with crossed orientation.

Serial photographs were compiled using Adobe Photoshop 5.5 (Adobe Systems, Inc., San Jose, CA, USA). The minimal model of the arculum *in situ* was composed in 3MAX V7.0 (Autodesk, San Rafael, CA, USA). For the sake of uniformity, we orient photographs with the distal end of the MET turned rightwards, the arculum or the rod from above. If necessary, originals were flipped.

Manipulation
We selected specimens that were able to respond with turns of the arculum upon manual extension of the tendon of the MET apodeme. Specimens were viewed under a Citoval 2 microscope (Carl Zeiss Jena, Jena, Germany), equipped with a Sigeta LCMOS 14,000 camera (Ningbo Haishu Honyu Opto-Electro Co., Ningbo, China) for video recording, with a frame rate of 10^{-1} s. Each specimen was submerged in 70% ethanol and gripped with two forceps: the first (immobile) held the proximal part of the apodeme, the second pulled the apodeme by the tibial ledge or its arthrodial membrane. An operator activated the arculum, moving the second forceps distally and proximally.

For a slow or stationary stretch of the tendon, we used an MM-1 micromanipulator with two clamps, which held a specimen in series with a loop of thin copper wire, glued to the tibial ledge, and a tungsten spring; this was oriented horizontally. For measurements, several referent points were selected on the tendon. Otherwise, a specimen was clamped by the MET apodeme in the vertical orientation, a loop was glued to the tibia, and loads were suspended under the loop (Fig. S3). Specimens were photographed under the MBS-9 microscope.

Videos were saved using the software ToupView 3.7.7158 (ToupTek Photonics Co., Hangzhou, China) and viewed with VirtualDub (Softtronic International, Barcelona, Spain). Each video was processed frame by frame using the software AVIEdit (AM Software, Moscow, Russia). Selected frames for illustrations were edited in Adobe Photoshop.

For distance measurements, each frame was loaded into the image window of Sigma Scan Pro (SPSS Inc., Chicago, IL, USA). Six to seven referent points were selected and clicked in each frame (Fig. S2). Coordinates were returned as a table in Excel format and processed by custom programs written in TurboBasic 1.3 (Borland International, Inc., Austin, TX, USA).

Referent points were projected onto a line that connected two grips, and distances from the midpoint of the cup (see Results, The MET apodeme) were calculated for all other points; hence a

computation problem was reduced to one dimension. Frame-by-frame positions of the arculum and the distal grip were analyzed and depicted using Excel.

Motile specimens of the MET apodeme were also actuated with pricks of an acupuncture needle close to the base of the arculum; imposed turns were video recorded. Another test, using motile specimens, recorded the ability of the arculum to turn upon stretch of the tendon; this test was performed after a local section of the tendon with a razor blade.

Videos were compressed or cropped using the AVIEdit software.

RESULTS

The femoro-tibial joint

The FTJ in beetles is bicondylar. Two condyles are situated on the anterior and superior faces of the tibia. Each condyle is fossed with a semicircular groove. Semicircular ridges inside the femur fit to grooves. Each set – consisting of the condyle, the groove and the ridge – forms a pivot for rotation of the tibia.

The distal edge of the femur overhangs the tibia. Its internal surface is invagination of the external cuticle. The dorsal proximal ledge of the tibia is hidden inside this invagination. The space between sclerotized counterparts of the femur and the tibia around the FTJ is protected with a sheath of the arthrodial membrane. This sheath is plicate in order to compensate for excursions of the tibia around pivots. The arthrodial membrane from the dorsal tibial ledge meets the dorsal membrane from the femur at some distance from the ledge.

These soft folds give origin for two deep invaginations (apodemes): one of the MET and another of the FCO. In addition, the arthrodial membrane above the dorsal tibial ledge houses (and presumably produces) an elastic tendon (*sensu* Weis-Fogh, 1960 or Burrows, 1987) between the tibia and the sclerotized part of the MET apodeme. The MET apodeme and the tendon form an integrated complex.

The MET apodeme

The apodeme of the m. extensor tibiae stretches proximally almost until the trochantero-femoral joint. This apodeme is composed of two unequal parts. Its proximal part is a stiff flat band, situated in the leg plane. Muscle fibers attach to both sides of the band. The band consists of numerous longitudinal sclerotized threads that are apparent when stripped of myofibrilla. Their number increases

distally, hence their distal mass seems dark brown. In Figs 3D,F, 4A,B and 9D, the distal part of the band (leftwards in each figure) appears in the frame. The band occupies over 80% of the integrated complex.

The transparent tendon occupies approximately 10% of the complex. Its shape is trapezoid, tapering proximally, and flattened in the plane, orthogonal to the band.

A compact transitional area exists between the band and the tendon. It consists of a strongly sclerotized cup-like body, convex distally. Some distal myofibrils attach to the proximal face of this cup. Arthrodial membranes, originated from the femur and from the tibia, couple together at the edge of the cup. The scheme of division is depicted in Fig. 2I.

As each invagination, this apodeme possesses the inverse order of cuticular layers, the outer empty space is instead saved inside as the central canal (Weis-Fogh, 1960). This canal is seen in macro photographs of the apodeme (Fig. 3F). Presumably, it initiates as a fold of the arthrodial membrane and tapers proximally. This expanded part of the canal above the tendon is designated below as the central funnel (see Figs 2F and 3B,D,F).

The FCO apodeme and the arculum

The neural part of the FCO in arcula-less beetles is situated at the base of the femur. A long rod-like apodeme joins the neural part with the dorsal ledge of the tibia. Its separate origin from the arthrodial membrane was found by us only in the blister beetles (Meloidae), including *Meloë proscarabaeus* (Fig. 2H). In other beetles, where apodemes were observed in detail, we found a long rod-like part of the FCO apodeme that emerged among the tendon (Fig. 2A–C, general view; D–F microphotographs) at various distances from the cup. The transparent rod in a small *Priacma serrata* (Archostemmata; Fig. 2G) also originates from the tendon.

The arculum in the Adephaga originates from the dorsal side of the tendon close to the cup (Fig. 3A). A soft ligament connects the tip with the FCO. The term ligament was applied earlier to soft threads connecting the FCO with femoral structures apart from the rod-like FCO apodeme (Usherwood et al., 1968; Bräunig, 1985). The arculum turns about its base upon stretching of the tendon.

The curved arculum in the Polyphaga bends the tendon around the anterior face of the tendon. The base of the arculum is situated on the dorsal side of the tendon, close to the cup (Fig. 3B,D–F). The
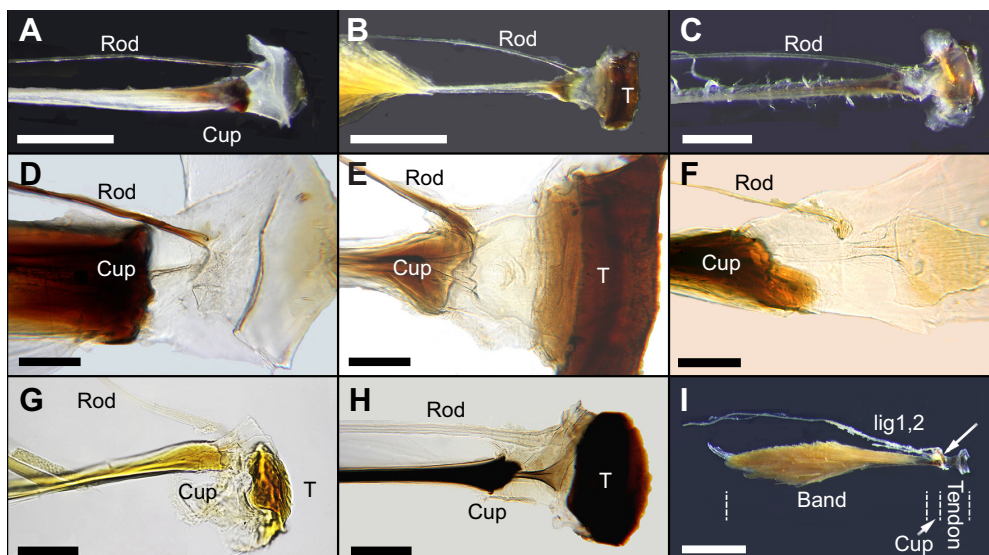

Fig. 2. Rods and ligaments of the FCO in five beetles without (and one with) arcula. Beetles with arcula: (A,D) *Hydrous piceus*, (B,E) *Prionus coriarius*, (C,F) *Zophobas atratus*, (G) *Priacma serrata* and (H) *Meloë proscarabaeus*. With arcula: (I) *Chalcophora mariana*. (A–C) Top view of the MET apodeme with the rod in front, (I) MET in *C. mariana*, dashed lines divide parts of the MET apodeme. (D–F) Origin of the rod from the tendon in beetles depicted in A–C; (G) origin of the rod presumably from the tendon; (H) top view of the tendon; (I) origin of two ligaments from the arculum (indicated with an arrow pointing downward). lig, ligaments to FCO; T, tibial ledge. Scale bars: (A,B,I) 1 mm, (C) 0.5 mm, (D,E,G,H) 0.2 mm, (F) 0.1 mm.
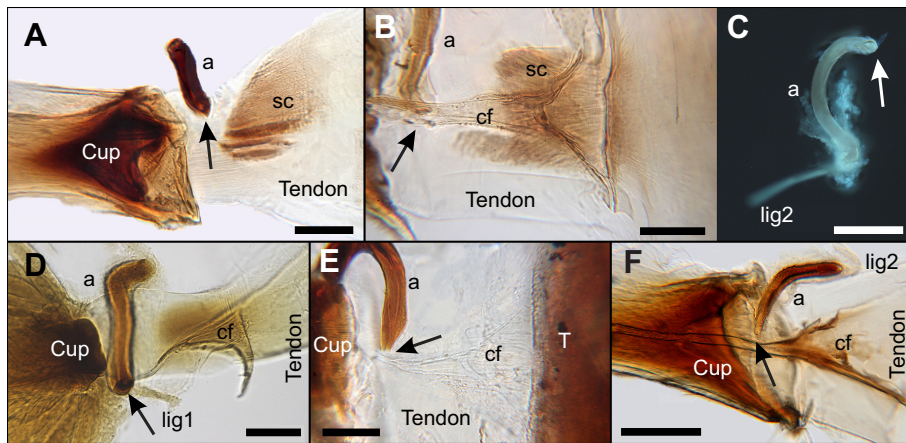
Fig. 3. Internal structures in the tendons of the MET. (A) *Carabus glabratus*, (B) *Melolontha melolontha*, (C,D) *Chalcophora mariana*, (E) *Lethrus apterus* and (F) *Lucanus cervus*. a, arculum; cf, central funnel; lig, ligaments to FCO; sc, internal sclerite; T, tibia. Base of the arculum is indicated with an arrow. Scale bars: (A,C,D,E) 100 μm, (B,F) 200 μm.

diameter of the base in the jewel beetle *Chalcophora mariana* (Fig. 3C) is approximately 15 μm; the hollow central canal, penetrating the base, is twice as narrow; and the chord of the arculum is 190 μm long. Traces of central canals are seen also in other beetles (Fig. 3B,D–F).

Polyphagan ligaments are complex. Usually they emerge as two branches – from the base (ligament 1) and from the tip of the arculum in *L. apterus* or *C. mariana* (ligament 2, remained after dissection in Figs 2I and 3C,F) – or divide into several branches distributed along the arculum, e.g. in some Scarabaeoidea (*Geotrupes* spp., *Oryctes nasicornis*) and in Coccinellidae. The FCO is often situated at the middle of the femur.

Four species of those that we inspected retained the ability of the arculum to rotate easily upon stretch or compression of the tendon after stripping and fixation in ethanol: *Calosoma inquisitor*, *L. apterus*, *Pentodon idiota* and *C. mariana*. We selected them as model species for manipulations.

Resilin in the MET apodeme

The brightest blue fluorescence upon ultraviolet excitation in a whole mount of the stripped MET apodeme in four model species

Fig. 4. Resilin in the MET apodeme. Distal parts of the MET viewed using (A,B) the light microscope and (C,D) the UV fluorescence microscope. (A,C) *Lethrus apterus*; (B,D) *Pentodon idiota*. Bright blue fluorescence is located in the tendon. Scale bars: (C) 200 μm, (D) 300 μm. a, arculum; lig2, ligament 2; T, tibia.

was observed in the tendon (Fig. 4). We assume that the tendon contains resilin.

Internal macrostructures in the tendon

The tendon appears transparent in most inspected beetles. However, we noticed narrow longitudinal strands in some large to giant beetles from old collections: dry (the ground beetle *A. mannerheimi* and the rhinoceros beetle *Megasoma elephas*), ethanol-fixed (the rhinoceros beetle *Allomyrina dichotoma*) or deep-frozen (the long-horn beetle *Prionus coriarius*). Strands are seen upon slant illumination; they either shine or look dark, depending on the angle of illumination (Fig. 5). This figure includes beetles with the arculum (Fig. 5A–C) as well as with a rod (Fig. 5D). The number of strands varies from a dozen to several dozen.

Two types of strands are recognized in the tendon of *M. elephas*: six wide goldish ones and many dark and thin ones among them (Fig. 5B, inset). At the distal edge of the cup, a palisade of elongated elements is evident; their spacing corresponds to the spacing of the strands. A similar palisade is seen in *A. dichotoma* (Fig. 5C, inset). The diameter of the palisade element in these beetles is 25–40 μm.

Brown sclerotized areas (Fig. 3A,B,D) are situated in the ventral part of the tendon. They occupy approximately one-third of the tendon. Sclerotizations were found in the carabids *Carabus glabratus*, *C. inquisitor* and *A. mannerheimi* (Fig. 5A), in *C. mariana* (Buprestidae) and in *Melolontha melolontha* (Scarabaeidae); however, they were not found in other inspected scarabs. Although amorphous in *M. melolontha*, sclerotization in carabids and *C. mariana* is organized as a fan of strands.

Imposed movements of the arculum

Manual stretch and release of the tendon with fine forceps has been filmed with a low frame frequency ($10\ \mathrm{s^{-1}}$) in four model species. In total, including other manipulations described in this section, we processed frame-by-frame 14 video fragments (of 39 total) containing 1074 frames (of 2514 total). Four compressed and cropped videos are available at http://izan.kiev.ua/ppages/frantsevich/arc.htm, or directly for *C. inquisitor* (Carabidae) at http://mail.izan.kiev.ua/frants/movie1_Inq.avi, *L. apterus* (Geotrupidae) at http://mail.izan.kiev.ua/frants/movie2_Leth.avi, *P. idiota* (Scarabaeidae) at http://mail.izan.kiev.ua/frants/movie3_Pen.avi, and *C. mariana* (Buprestidae) at http://mail.izan.kiev.ua/frants/movie4_Chal.avi.

The arculum is pivoted at its base and rotates around the axis perpendicular to the leg plane, and the tip turns distally upon stretch of the tendon, as shown frame-by-frame in *P. idiota* in Fig. 6.
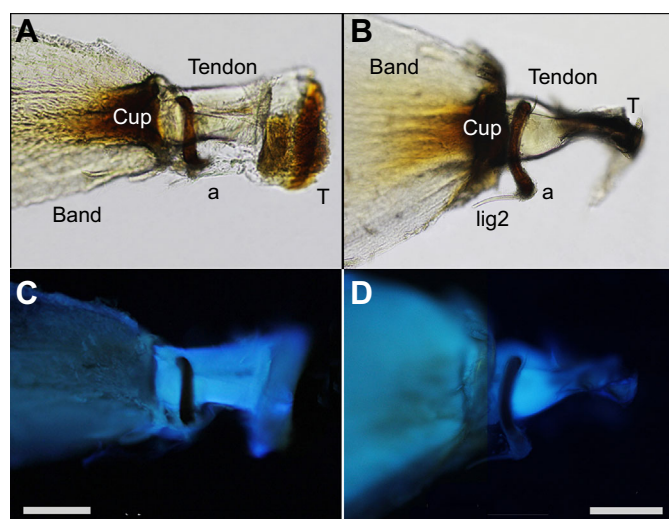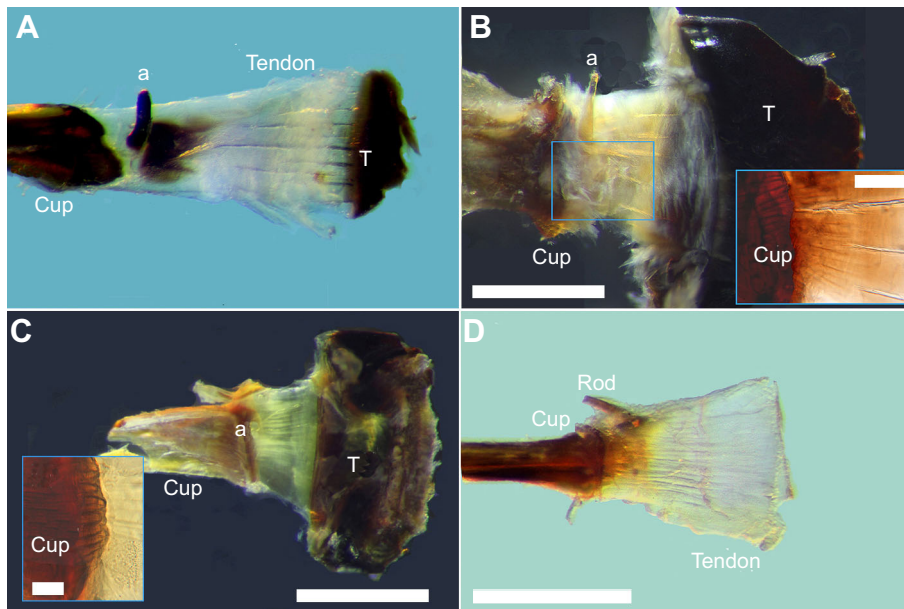
Fig. 5. Fan-like strands inside the tendons. (A) *Anthia mannerheimi*, (B) *Megasoma elephas*, (C) *Allomyrina dichotoma*, (D) *Prionus coriarius*. Strands connect the cup with the tibia. Connection is shown in insets in B and C. Scale bars: (B,C) 1 mm, (A,D) 0.5 mm, (B inset) 250 µm, (C inset) 100 µm. The distal stump of a rod-like FCO apodeme is abbreviated as rod. a, arculum; T, tibia.

We analyzed projections of the relevant points onto the force vector between two grips and counted distances between projections. Plots in Fig. 7 compare 1D positions of the tip of the arculum versus its base, the distal tendon border or the tibial ledge. Synchrony is evident for turns of the tip of the arculum and stretching of the tendon. Plots show how oscillations of the tip of the arculum amplify displacements at its base (Fig. 7C,D). The best amplification was achieved in *L. apterus* (Fig. 7B); oscillations of the arculum were broader than applied stretch–release at the distal tendon border.

Table S3 shows correlation coefficients between synchronous shifts of relevant points: the tip and base of the arculum, the tips of gripping forceps, the distal edge of the tendon or the tibial ledge. Distances were measured from the cup. Correlations between the tip and distal relevant points were mostly significant. Correlations between oscillations of two grips were mostly low. The base of the arculum moved so slightly with respect to the cup that its synchrony with the applied stretch vanished in errors of pixelization.

The relative amount of stretch–release was evaluated in videos in which the steady distal drift of the grip by the slippery tibia was absent. The total duration of 11 fragments comprised 805 frames. We measured displacement of the distal grip relative to the cup. On average, the span of stretch–release was approximately 30% of the mean length of the tendon, with extreme values of 59% and 12%.

Also, we tested responses to a local deformation of the tendon close to the base of the arculum in *P. idiota*. We held a specimen by the band with the forceps, pricked the tendon with an acupuncture needle and video recorded turns of the arculum. Two successful videos were analyzed (in total 718 frames). Selected frames of pricking distally, laterally or proximally from the base during one cycle of manipulation are shown on Fig. 8. Respectively, the tip turned proximally, dorsally or distally, i.e. against piercing.

Lastly, we prepared specimens of the stripped MET apodeme from *L. apterus* and *P. idiota*, which are able to respond with turns of the arculum to the manual stretch of the tendon. We cut a shallow incision close to the base of the arculum, across or along the dorsal face of the tendon. Incisions cut distally, anteriorly or posteriorly from the base, did not prevent turns of the arculum. However, the incision between the base and the cup prevented turns of the arculum in 13 of 13 specimens of *L. apterus* and
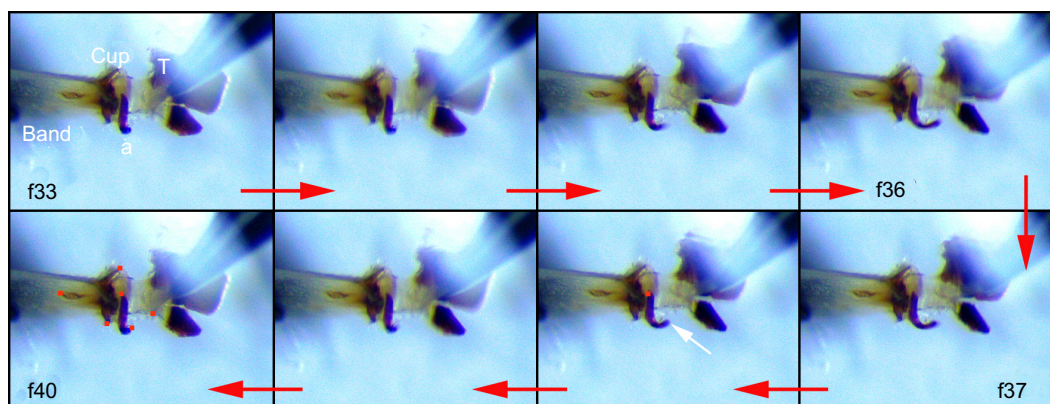

Fig. 6. Manipulated turn of the arculum in *Pentodon idiota* (eight frames from one cycle of stretch–release). Frames (f33 to f40) are arranged cyclically, with a frame rate of 10 s^{-1}. The length of the tendon is minimal in f33 and f40, maximal in f36 and f37. Positions of the base and the tip of the arculum are indicated with a red dot and a white arrow in f38. The neutral position is shown in f33 and f40. Reference points are indicated with red dots in f40. a, arculum; T, tibia.
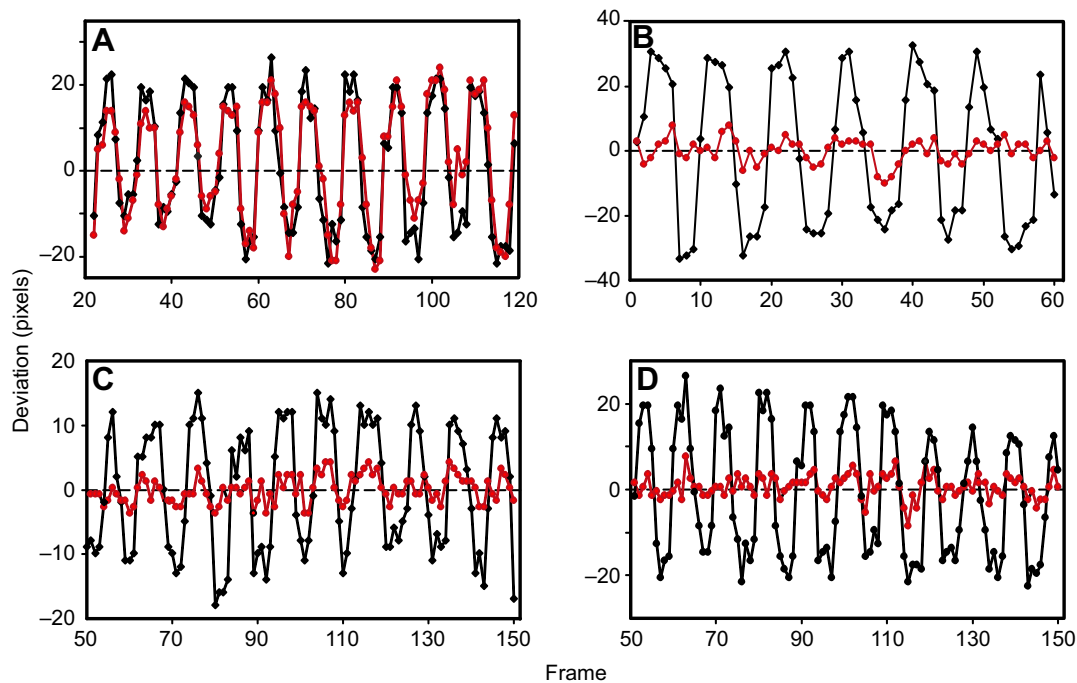
Fig. 7. Oscillations of the tip of the arculum (black) and other relevant points (red) during manual stretch–release of the tendon. (A,D) *Pentodon idiota*, excerpts of total 172 frames; (B) *Lethrus apterus* and (C) *Calosoma inquisitor*, excerpts of total 173 frames. Relevant points are (A) grip of the movable forceps (correlation with the tip 0.947); (B) distal edge of the tendon (correlation 0.523); (C) base of the arculum (correlation 0.668); (D) base of the arculum (correlation 0.898). *y*-axis shows deviations from mean projections on the line between two grips (in pixels).

P. idiota; the arculum only translated a bit distally upon stretching of the tendon. The transverse incision in the ventral face of the tendon just distally to the cup did not affect turns of the arculum in a capable specimen.

Attempts to exert any imposed movements in a short stump (i.e. the basal part) of the rod in the arculum-less *Hydrous piceus* and *Zophobas atratus* by stretching of the tendon were ineffective.

Forces in the MET tendon

Experiments were performed on glycerol-soaked specimens of *L. apterus*. Horizontal stretch of the tendon in series with a coil spring allows to pull the tendon smoothly and fix the tendon in the necessary position (Fig. S3). We exerted a slow turn of the arculum until its limit and left the specimen for an indefinite time period. On

the one hand, we get certain that the arculum after a stepwise turn did not return exponentially to its neutral position – in a specimen devoid of myofibrils or other viscous components. On the other hand, we could measure extension of the tendon by relevant points on photographs. Using two pairs of relevant points, we evaluated the average length of the unloaded tendon as 0.28 mm, its width as 0.25 mm and the constant volume of the cylinder of such size as 0.01226 mm^3.

At the utmost turn, the length was 0.32 mm, 1.14 times greater relative to the initial state. Elongation, or change in length, was 0.14-fold. Elongation is proportional to applied force (Alexander, 1968). Using the value of Young's modulus for resilin of 1.8 MPa (Alexander, 1968, table 3) and the cross-section of elongated tendon of 0.038 mm^2, or 3.8×10^{-8} m^2, we
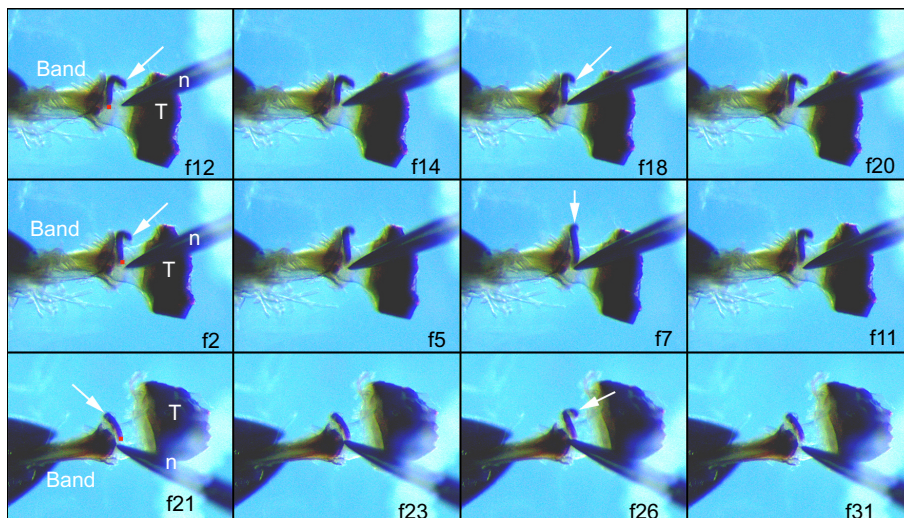

Fig. 8. Turns of the arculum upon local pricking with a needle close to the base of the arculum in *Pentodon idiota* (numbered video frames). Top row: pricking distally to the base, leg L1; middle row: pricking laterally to the base, same leg; bottom row: pricking proximally to the base, leg R3. No pricking in the first and fourth columns, maximal deformation in the third column. The tip of the arculum rotates proximally (top row), dorsally (middle row) and distally (bottom row). The base of the tibia is indicated with a red dot in the left column; positions of the tip are indicated by white arrows. n, needle; T, tibia.
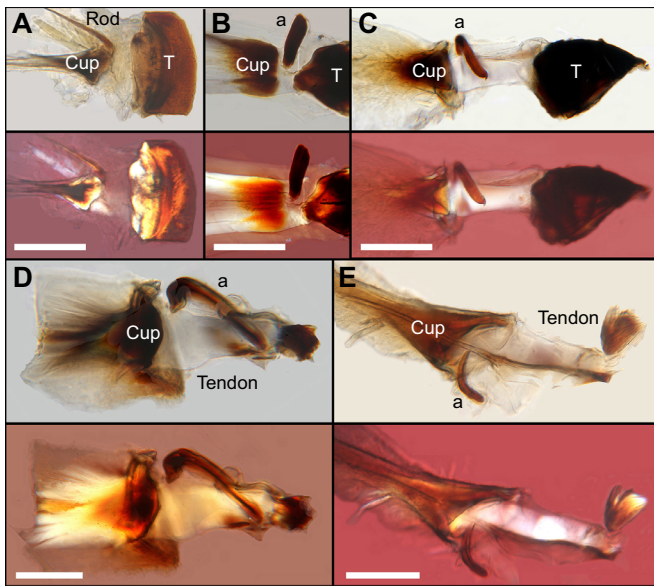
Fig. 9. Optical activity in the MET apodeme. Polaroids stay in parallel (odd rows) or are crossed (even rows). (A) *Prionus coriarius*, (B) *Anthia mannerheimi*, (C) *Lethrus apterus*, (D) *Pentodon idiota* and (E) *Lucanus cervus*. Note the following: (1) opacity in transparent tissues between parallel polaroids corresponds to bright areas between crossed polaroids; (2) dark-brown sclerotized areas of the cup or of the tibial ledge between parallel polaroids appear shining between crossed polaroids; (3) the arculum always appears dark brown. Scale bars: (A) 500 μm, (B,E) 300 μm, (C,D) 200 μm. a, arculum; T, tibia.

obtained a value of force per this area of 0.0096 N, approximately 0.01 N, equal to a weight of approximately 1 g. Weis-Fogh (1960) originally indicated a wider range of the modulus of 0.5–3 MPa.

Preparation of specimens included two destructive episodes of desiccation: sticking to a rubber scaffold and sticking of a loop, with further recovery in 70% ethanol or glycerol. The most sensitive specimen in the vertical suspension (Fig. S3C,D) demonstrated almost complete turns of the arculum upon loads of 0.005–0.01 N.

Measurements of levers in tibiae of *L. apterus* revealed a ratio between internal (proximal to pivots) and external levers (distal to pivots) of 1 to 11.7, on average. Hence, forces applied to the tibio-tarsal joint must be less than 0.001 N in order to exert the full turn of the arculum.

Optical activity in the MET apodeme

We photographed whole mounts of the MET, embedded in the glycerol–chloral hydrate–gum medium, between two polaroids in parallel or in crossed positions. Exposure time between crossed polaroids was at least 10-fold longer than between parallel ones. Achromatic whole mounts revealed three optical effects (Fig. 9). (1) Empty background appears bright between parallel polaroids and becomes dark purple between crossed polaroids because of residual color transmission. (2) Transparent areas in the tendon look as bright as the background without polaroids, shaded between parallel polaroids, and brighter than the background between crossed filters. (3) Sclerotized structures look brown or dark brown without polaroids or between parallel polaroids. Some of them still look dark between crossed polaroids [arcula in all specimens, the tibial ledge in Fig. 9B,C,D (*A. mannerheimi*, *L. apterus*, *P. idiota*) and the cup in Fig. 9C,E (*L. apterus*, *L. cervus*)]. In other specimens, pieces of the ledge and the cup shine brightly between crossed polaroids.

Effects 2 and 3 manifest optical activity in biological materials, i.e. rotation of the polarization plane. If a sclerotized structure is inactive, its sign of contrast against the background does not change upon rotation of one polaroid. In heavily sclerotized structures, the transmitted light is so low that the contrast effect disappears.

DISCUSSION

Simplest model of a mechanical amplifier

In this experimental study, we reduced the mechanism that moves the arculum to three components: the tendon, the arculum and the cup. When the cup is fixed and the tendon is stretched, the tip of the arculum turns distally, whereas displacement of the base of the arculum is small.

The model is proposed on the basis of the following structural or dynamical facts: (1) the arculum is attached to the dorsal side of the tendon, at a small, but non-zero distance from the cup; (2) the arculum is a part of the apodeme with a central canal inside, hence the attachment area is not punctual (see a hoof-like base of the arculum in Fig. 3C); (3) the tendon is elastic; deformations in the whole tendon are unidirectional; (4) the tip of the arculum turns distally upon stretching of the tendon (Fig. 6 and videos listed in the Results, Imposed movements of the arculum); (5) local deformations (pricking) of the tendon near the base of the arculum exert turns of the arculum; and (6) local destruction of the link between the base and the cup prevents rotation of the arculum.

Consequently, (7) the center of the base rotation cannot be inside the base, because all points in the base move in the same direction; (8) a non-stretched link 'base-cup' attaches to the base tangentially; and (9) crossing between the arculum and the tendon is impossible. The above conditions are satisfied if: (10) the axis of rotation of the arculum is (approximately) perpendicular to the leg plane and (11) touches the base at its extreme dorsal point; and (12) the base of the arculum inserts at some depth into the tendon, (13) but the dorsal edge of the base is tied with the cup with a non-stretched or hardly stretched link. The scheme of the model is depicted in Fig. 10.

Structures in the tendon

The tendon of the MET in beetles is transparent and elastic. Elasticity and blue fluorescence upon UV illumination are compatible with the
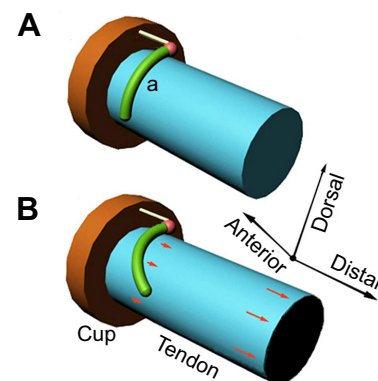

Fig. 10. Scheme of rotation of the arculum, actuated by stretch of the tendon. (A) Position of the arculum before stretch and (B) after stretch. A minimal model consists of the cup, the tendon and the arculum (green body, labeled with 'a'), situated closely to the cup. The model is turned to the viewer with its anterior face. The base of the arculum is depicted as a red ball. The axis of arculum rotation (not depicted) is oriented anteriorly and touches the base from above. A white line symbolizes a non-stretched link between the base and the cup.

properties of resilin. Resilin has been investigated in many superficial structures: tarsal setae, arthrodial membranes, the cornea of the compound eye, and wing membranes (Mishels et al., 2016; Haas et al., 2000a,b). The specific fluorescence of resilin was recorded in tendons of the MET apodeme in jumping legs of flea beetles (Crysomelidae: Alticinae) (Nadein and Betz, 2016, fig. 12) and of the weevil *Orchestes fagi* (Curculionidae) (Nadein and Betz, 2018, fig. 8). The presence of resilin inside cursorial, swimming and digging legs in beetles has not been recorded before.

The initial functions of resilin in tibial muscles are, presumably, to damp collisions with obstacles during locomotion and digging, for example, and to save energy for reverse motions. A particular function of resilin in the MET is participation in the sensory signal transmission to the FCO.

Resilin-containing formations are composite structures made of loose protein chains and chitin fibers oriented in order. The size of chitin fibers covers a great range from nano- to macro-structures. The length of an elementary chitin nanofiber is 0.3 µm with a diameter of 3 nm (Vincent and Wegst, 2004). Weis-Fogh (1960) found chitin lamellae inside resilin formations; their diameter was less than 200 nm and the spacing was 2–3 µm. The diameter of chitin fibers in Maulik's spring – an equivalent of the cup in flea beetles – was 50–100 nm (Furth et al., 1983).

Exocuticular chitin fibers in the pliable arthrodial membrane of a dragonfly's neck were approximately 30 nm in diameter, with a length of approximately 0.5 µm and spacing between fibers of 10–100 nm (Gorb, 2000). Spacing between lamellae inside the resilin–chitin composite allows them to slide freely over each other (Gorb, 2000). The structure of resilin–chitin composites, of which the cutucular component was claimed to be an accumulator of deformation energy, has not been investigated until now, in locusts (Burrows, 2016), fleas (Siphonaptera) and hemipterans (Cercopidae and Fulgoridae) (referred to in Burrows and Sutton, 2012), and mantis shrimp (Crustacea: Stomatopoda) (Patek et al., 2013).

We observed several sclerotized macrostructures inside the tendon. Firstly, we observed sclerotized areas at the ventral face of the tendon (in large and medium sized carabids, and in *M. melolontha* and *C. mariana*). These formations occupy areas of $n\times100$ µm in length and width. Their probable purpose is strengthening of the ventral tendon face against a stiff contact with the tibial ledge, when the tibia is flexed. Secondly, we observed strands along the whole tendon in large and giant beetles. The length and spacing of strands was 500–700 µm and 70–100 µm in *A. mannerheimi*, 700–900 µm and 150–200 µm for wide strands and 20–50 µm for thin strands in *M. elephas*, 400–500 µm and 30–40 µm in *A. dichotoma*, and 600 µm and 30–50 µm in *P. coriarius*. Regretfully, we observed old specimens, which had been stored for years; thus we could not determine whether tendons in these species would have been stretchable *in vivo*. Shumakova (1990a) reported the presence of sclerotized lamellae (possibly strands in cross-section) in the tendon of *L. apterus*. It is difficult to fit a stretchable tendon with flat chitinous strands, which are resistant to stretch. Finally, we noticed an intriguing structure in the cups of giant rhinoceros beetles (Dynastinae: Scarabaeidae; Fig. 5, insets): densely packed parallel fibers (diameter 30–50 µm), which are oriented along the proximal–distal axis of the femur and end exactly at the border between the cup and the tendon.

FCOs with the arcula may compete with dipteran halters in their mechanical complexity. We hope that the story of the arcula, described above, is not finished yet, but will attract the attention of entomologists and physiologists to the evolution of FCOs among beetles, to the mechanical properties of the FCO apodeme and its surround, and to processing of the signal from the arculum by scoloparia in the FCO.

Author contributions
Conceptualization: L.F.; Methodology: L.F., I.S., D.G.; Software: L.F., D.G.; Formal analysis: L.F.; Investigation: L.F., I.S., D.G.; Writing - original draft: L.F., I.S.; Writing - review & editing: L.F., D.G.; Visualization: L.F., I.S., D.G.; Project administration: L.F.

References
Alexander, R. M. (1968). *Animal Mechanics*. London: Sidgwick and Jackson.

Bässler, U. (1965). Proprioreceptoren am Subcoxal- und Femur-tibia-Gelenk der Stabheuschrecke *Carausius morosus* und ihre Rolle bei der Wahrnehmung der Schwerkraftrichtung. *Kybernetik* **2**, 168-193. doi:10.1007/bf00272558

Bässler, U. (1967). Zur Regelung der Stellung des Femur-Tibia-Gelenkes bei der Stabheuschrecke *Carausius morosus* in der Ruhe und im Lauf. *Kybernetik* **4**, 18-26. doi:10.1007/BF00288822

Brankov, G. (1981). *Basics of Biomechanics (in Russian)*. Moscow: Mir.

Bräunig, P. (1985). Strand receptors associated with the femoral chordotonal organs of locust legs. *J. Exp. Biol.* **116**, 331-341.

Burns, M. D. (1974). Structure and physiology of the locust femoral chordotonal organ. *J. Insect Physiol.* **20**, 1319-1339. doi:10.1016/0022-1910(74)90236-4

Burrows, M. (1987). Parallel processing of proprioceptive signals by spiking local interneurons and motor neurons in the locust. *J. Neurosci.* **7**, 1064-1080. doi:10.1523/JNEUROSCI.07-04-01064.1987

Burrows, M. (2016). Development and deposition of resilin in energy stores for locust jumping. *J. Exp. Biol.* **219**, 2449-2457. doi:10.1242/jeb.138941

Burrows, M. and Sutton, G. P. (2012). Locusts use a composite of resilin and hard cuticle as an energy store for jumping and kicking. *J. Exp. Biol.* **215**, 3501-3512. doi:10.1242/jeb.071993

Field, L. H. and Matheson, T. (1998). Chordotonal organs of insects. *Adv. Insect Physiol.* **27**, 1-228. doi:10.1016/S0065-2806(08)60013-2

Frantsevich, L. I. and Shumakova, I. D. (1985). Arcular chordotonal organ in Coleoptera (in Russian). *Rep. Acad. Sci. USSR* **282**, 469-473. (http://mail.izan. kiev.ua/frants/DAN.pdf).

Frantsevich, L. I. and Shumakova, I. D. (1987a). Biomechanics of the arcular apparatus in the arcular chordotonal organ in beetles (Insecta, Coleoptera) (in Russian). *Sens. Syst.* **1**, 39-46. (http://mail.izan.kiev.ua/frants/Biom.pdf).

Frantsevich, L. I. and Shumakova, I. D. (1987b). Evolution of structure and function of the arcular apparatus in beetles (Coleoptera) (in Russian). *Entomol. Rev.* **66**, 735-745. (http://mail.izan.kiev.ua/frants/EnRev.pdf and http://mail.izan. kiev.ua/frants/Plates.pdf).

Frantsevich, L. I. and Shumakova, I. D. (1993). The luxury of evolution: elaborated structure without evident function. In *Sensory Systems of Arthropods* (ed. K. Wiese, F. G. Gribakin, A. V. Popov and G. Renninger), pp. 670-674. Basel, Boston, Berlin: Birkhauser Verlag. (http://mail.izan.kiev. ua/frants/Biona.pdf).

Furth, D. G., Traub, W. and Harpaz, I. (1983). What makes *Blepharida* jump? a structural study of the metafemoral spring of a flea beetle. *J. Exp. Zool.* **227**, 43-47. doi:10.1002/jez.1402270107

Gorb, S. N. (2000). Ultrastructure of the neck membrane in dragonflies (Insecta, Odonata). *J. Zool. Lond.* **250**, 479-494. doi:10.1111/j.1469-7998.2000.tb00791.x

Haas, F., Gorb, S. and Blickhan, R. (2000a). The function of resilin in beetle wings. *Proc. Roy. Soc. Lond. B Biol. Sci.* **267**, 1375-1381. doi:10.1098/rspb. 2000.1153

Haas, F., Gorb, S. and Wootton, R. J. (2000b). Elastic joints in dermapteran hind wings: materials and wing folding. *Arthropod Struct. Dev.* **29**, 137-146. doi:10. 1016/S1467-8039(00)00025-6

Heitler, W. J. (1974). The locust jump: specialisations of the metathoracic femoraltibial joint. *J. Comp. Physiol.* **89**, 93-104. doi:10.1007/BF00696166

Kent, K. S. and Griffin, L. M. (1990). Sensory organs of the thoracic legs of the moth *Manduca sexta*. *Cell Tissue Res.* **259**, 209-223. doi:10.1007/BF00318442

Michels, J., Appel, E. and Gorb, S. N. (2016). Functional diversity of resilin in Arthropoda. *Beilstein J. Nanotechnol.* **7**, 1241-1259. doi:10.3762/bjnano.7.115

Nadein, K. and Betz, O. (2016). Jumping mechanisms and performance in beetles. I. Flea beetles (Coleoptera: Chrysomelidae: Alticini). *J. Exp. Biol.* **219**, 2015-2027. doi:10.1242/jeb.140533

Nadein, K. and Betz, O. (2018). Jumping mechanisms and performance in beetles. II. Weevils (Coleoptera: Curculionidae: Rhamphini). *Arthropod Struct. Dev.* **47**, 131-143. doi:10.1016/j.asd.2018.02.006

Patek, S. N., Rosario, M. V. and Taylor, J. R. A. (2013). Comparative spring mechanics in mantis shrimp. *J. Exp. Biol.* **216**, 1317-1329. doi:10.1242/jeb.078998

Shelton, P. M. J., Stephen, R. O., Scott, J. J. A. and Tindall, A. R. (1992). The apodeme complex of the femoral chordotonal organ in the metathoracic leg of the locust *Schistocerca gregaria. J. Exp. Biol.* **163**, 345-358.

Shumakova, I. D. (1989). Electrophysiological study of the arcular chordotonal organ in the beetle femur (in Russian). *J. Evol. Biochem. Physiol.* **5**, 670-674. (http://mail.izan.kiev.ua/frants/Elphys.pdf).

Shumakova, I. D. (1990). Histological study of the arcular chordotonal organ in the beetle femur (in Russian). *J. Evol. Biochem. Physiol.* **3**, 427-429. (http://mail.izan. kiev.ua/frants/Histo.pdf).

Shumakova, I. D. (2003). Peculiar construction of the femoral chordotonal organ in some beetles (Coleoptera) and the suspended sclerite of the extensor tibiae in bugs (Hemiptera) (in Russian). *Vestn. Zool.* **10** Suppl., 164-170. (http://mail.izan. kiev.ua/frants/bugs.pdf).

Slifer, E. H. (1935). Morphology and development of the femoral chordotonal organs of *Melanoplus differentialis* (Orthoptera, Acrididae). *J. Morph.* **58**, 615-637. doi:10. 1002/jmor.1050580212

Usherwood, P. N. R., Runion, H. I. and Campbell, J. I. (1968). Structure and physiology of a chordotonal organ in the locust leg. *J. Exp. Biol.* **48**, 305-323.

Vincent, J. F. V. and Wegst, U. G. K. (2004). Design and mechanical properties of insect cuticle. *Arthropod Struct. Dev.* **33**, 187-199. doi:10.1016/j.asd.2004. 05.006

Weis-Fogh, T. (1960). A rubber-like protein in insect cuticle. *J. Exp. Biol.* **37**, 889-907.